

1     **Geometry and topology of Polish Outer Carpathian digital**  
2     **elevation model interpreted lineament network in context of**  
3                     **regional tectonics**

4     Maciej Kania<sup>1</sup>, Mateusz Szczęch<sup>1</sup>

5     <sup>1</sup>Jagiellonian University in Kraków, Faculty of Geography and Geology, Institute of Geological Sciences,  
6     Gronostajowa 3a, 30-863 Kraków, Poland

7     *Correspondence to:* Maciej Kania (maciej.kania@uj.edu.pl)

8

9 **Abstract.** The Polish part of the Western Outer Carpathians lineament network was analysed based on the  
10 GMTED2010 digital elevation model. Lineaments were identified in the visual screening of the hillshade model.  
11 To the best of our knowledge, no one has studied the geometrical properties of the network with relation to the  
12 topological ones. The NetworkGT QGIS toolbox was applied to identify the nodes and branches of the network,  
13 as well as to calculate the topology parameters. Our aim was to find differences between the western and eastern  
14 parts of the Western Outer Carpathians; therefore, the analyses were carried out in six sectors chosen based on  
15 the geographical subdivision in the geological context: three in the north, mainly the Silesian unit; and three in  
16 the south, mainly the Magura unit. We found general agreement of the identified network with the  
17 photolineament map; however, some of the photolineaments are not confirmed by digital elevation model  
18 (DEM). We found that the topological parameters of the networks change from west to east, but not from north  
19 to south. There are areas of increased interconnectivity, especially the Nowy Sącz Basin, where the lineament  
20 network may reflect a complicated system of cross-cutting deep-rooted fault zones in the basement.

## 21 **1. Introduction**

22 Remote sensing imagery is an important source of data in regional tectonics, and its importance has been  
23 growing in recent years. Since the 1970s, there have been multispectral satellite photos of the Earth surface  
24 applied mainly in mineral mapping (e.g. van der Meer et al., 2012), as well as in tectonic studies (e.g. Leech et  
25 al., 2003). The Shuttle Radar Topography Mission (SRTM) resulted in the first remote sensing digital elevation  
26 model of most of the continental surface of the planet, with immense potential for application in geology (Yang  
27 et al., 2011). Then, new superior resolution and quality models were created on both the global (satellite) and  
28 local scale (mainly airborne LiDAR scanning). Digital elevation models are especially useful in areas with lush  
29 vegetation. The application of LiDAR in the Carpathians' flysch-type mountains in geological interpretations  
30 was shown, for example, in Kania and Szczęch (2022).

31 Our previous study (Kania and Szczęch, 2020), based on the interpretation of the model augmented with field  
32 geological mapping (Szczęch and Cieszkowski, 2021), showed how a lineament network can be interpreted in  
33 topological and geometrical terms. The aim in the present paper is to up-scale DEM-based geometrical and  
34 topological analyses of a regional scale lineament network to find how this is reflected in the tectonic structure  
35 of the Western Carpathians. Previous studies of the Carpathian lineaments were mainly focused on lineament  
36 strikes distribution (e.g. Doktor and Graniczny, 1982, 1983; Doktor et al., 1985, 1990, 2002; Bażyński et al.,  
37 1986; Graniczny and Mizerski, 2003); therefore, we decided to add an interconnectivity aspect in terms of the  
38 topological parameters (Valentini et al., 2007; Sanderson and Nixon, 2015; Thiele et al., 2016), as a way of  
39 better understanding the structural problems. Most of the Carpathian-related studies are geographically organised  
40 in mountain arc parallel belts, reflecting the main tectonostratigraphic units, now forming nappes and being  
41 sedimentary basins during the Carpathian flysch depositions. We decided to keep this subdivision, although  
42 combining this with physiographical subdivisions into sectors with borders perpendicular to the Carpathian belt.

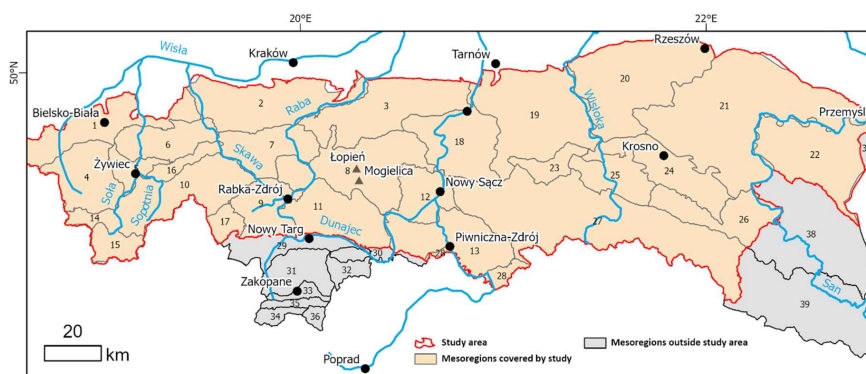
## 43 **2. Up-to-date research on the Polish Outer Carpathian lineaments**

44 The fact that dislocation lines perpendicular to the Carpathian arc are related to the deep basement, and are  
45 significantly older than the Carpathians themselves, was postulated even before the remote sensing era  
46 (Teisseyre, 1907). The first modern attempts to interpret lineaments in the Polish Carpathians were based on the  
47 Landsat MSS imagery and Heat Capacity Mapping Mission satellite, and reported together with data from the

48 whole territory of Poland on a photogeological map at 1:1 000 000 scale ([Bażyński et al., 1986](#); Graniczny and  
 49 Mizerski, 2003; [Bażyński et al., 1986](#)). The main lineament systems of the Western Carpathians in the context of  
 50 structural geology were shown by Doktor and Graniczny (1983) and Doktor et al. (1985). The results of satellite  
 51 imagery lineament detections were then correlated with geophysical data proving relationships between the  
 52 surface, neotectonic processes and deep Carpathian basement structure ([Motyl-Rakowska and Ślaczka, 1984](#);  
 53 Doktor et al., 1990; [Motyl-Rakowska and Ślaczka, 1984](#)). Airborne radar data were applied in tectonic analysis  
 54 of the Carpathians, resulting in 17 000 short lineaments that were the basis of the lineament density map (Doktor  
 55 et al., 2002). The interpretation of SRTM hillshading visualisation was performed by Chodyń (2004) on the  
 56 limited area in Beskid Wyspowy Mts. Comparison of Landsat MSS and SRTM data by Ozimkowski (2008)  
 57 showed that whilst the main faults can be related to lineaments, there are still numerous lineaments without  
 58 geological explanation.

### 59 3. Study area

60 The choice of the study area was based on the physiogeographical subdivision of Poland by Solon et al. (2018).  
 61 The following macroregions were selected: the Western Beskidy Foothills, Western Beskidy Mts., Orawa-  
 62 Podhale Basin, Mid-Beskidy Foothills and Mid-Beskidy Mts. ([Fig. 1](#)). These five regions, with a total area of  
 63 17 437 km<sup>2</sup>, cover most of the Polish part of the Outer Carpathians, excluding a small part of the Eastern Outer  
 64 Carpathians located in Poland.



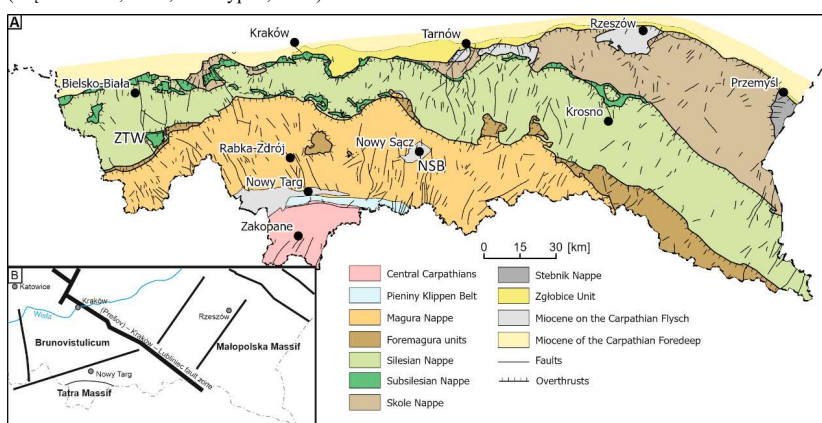
67 **Fig. 1. Physiogeographical subdivision of the study area (beige colour) and adjanted parts of the Polish**  
 68 **Carpathians based on Solon et al. (2018), Mesoregions covered by study: 1 – Silesia Foothills, 2 –**  
 69 **Wieliczka Foothills, 3 – Wiśnicz Foothills, 4 – Silesian Beskid Mts, 5 – Żywiec Basin, 6 – Mały Beskid Mts,**  
 70 **7 – Makowski Beskid, 8 – Wyspowy Beskid, 9 – Orawa-Jordanów Foothills, 10 – Żywiec-Orawa Beskid**  
 71 **Mts, 11 – Gorce Mts, 12 – Sącz Basin, 13 – Sącz Beskid Mts, 14 – Koniaków Intermontane Region, 15 –**  
 72 **Żywiec-Kysuce Beskid Mts, 16 – Pewel-Krzeczów Ranges, 17 – Orawa Interfluve, 18 – Rożnów Foothills,**  
 73 **19 – Cieczkowice Foothills, 20 – Strzyżów Foothills, 21 – Dvńów Foothills, 22 – Przemyśl Foothills, 23 –**  
 74 **Gorlice Basin, 24 – Jasło-Krosno Basin, 25 – Jasło Foothills, 26 – Bukowiec Foothills, 27 – Low Beskid**  
 75 **Mts, 28 – Poprad Foothills; mesoregions outside the study area: 29 – Orawa-Nowy Targ Basin, 30 –**  
 76 **Pieniny Mts, 31 – Fore-Tatra Foothills, 32 – Magura Spiska Mts, 33 – Sub-Tatra Depression, 34 – Western**

- sformatowano: Czcionka: Pogrubienie
- sformatowano: Czcionka: Pogrubienie
- sformatowano: Angielski (Zjednoczone Królestwo)

77 [Tatra Mts, 35 – Reglowe Tatra Mts, 36 – High Tatra Mts, 37 – Hermanowice Submontane Region, 38 –](#)  
78 [Sanocko-Turczańskie Mts, 39 – Bieszczady Mts.](#)

### 80 3.1 Geological setting of the study area

81 The research area is located in the Polish sector of the Western Outer Carpathians (Mahel', 1974; Książkiewicz, 1977; Ślącza et al., 2006; Fig. 42). It contacts tectonically with the Pieniny Klippen Belt from the south, which is a border between the Outer and the Central Carpathians (Książkiewicz, 1977; Plašienka, 2018; Golonka et al., 2019a, 2020, 2021, 2019b; Książkiewicz, 1977). The basement under the Western Outer Carpathians is formed of two blocks: Brunovistulicum and Małopolska Massif, which are separated by major tectonic zone: Kraków – Lubliniec Fault (Fig. 2B) Żaba, 1999; Żelaźniewicz, 2011), cut by numerous other deep rooted lineaments (Doktór, 1985). The Outer Carpathians are built mainly of flysch deposits, whose thickness is approximately 6 000 m, and thus they are also referred to as the Flysch Carpathians (Książkiewicz, 1977; Golonka et al., 2005, 2021; Golonka et al., 2020; Ślącza et al., 2006; Golonka et al., 2005; Książkiewicz, 1977). These deposits are Late Jurassic–Early Miocene in age and are mainly deep-sea sediments deposited by the gravity flow in the several sedimentary basins of the Northern Tethys, separated by ridges (Książkiewicz, 1977; Golonka et al., 2005, 2020, 2021; Ślącza et al., 2006; Książkiewicz, 1977). The thrust of the Central Carpathians block to the north on the European Platform blocks — the Brunovistulicum and Małopolska Massif (Żaba, 1999) — led to the forming of the synorogenic stage accretionary prism. The sediments deposited in the basins were folded and thrust one upon another, creating the sequence of the nappes in the Miocene. Going from the south there are the Magura Nappe, Dukla Nappe, Fore–Magura group of nappes, Silesian Nappe, Sub-Silesian Nappe and Skole Nappe (Mahel', 1974; Książkiewicz, 1977; Golonka et al., 2005, 2019a; Ślącza et al., 2006). The deposits of the Outer Carpathians are overthrust on the Miocene molasses filling the Carpathian Foredeep, which was deposited on the front of the Outer Carpathian orogenic belt thrusting over the North European Platform (Ślącza et al., 2006; Oszczytko, 2006).

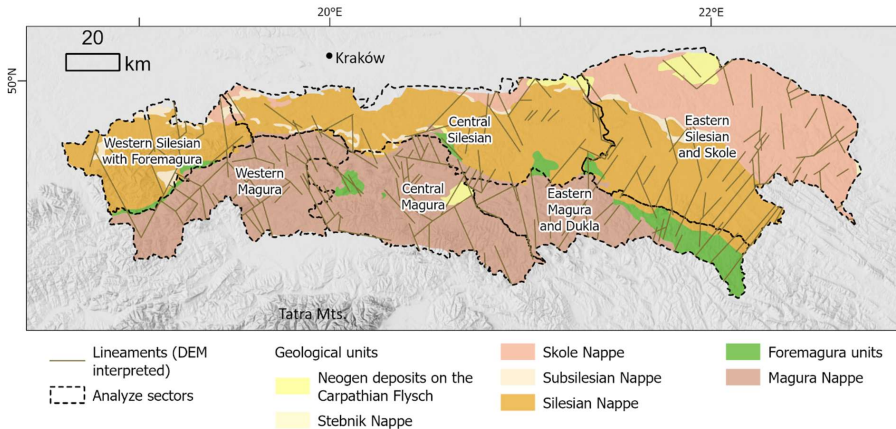


101 **Fig. 42. A:** Generalised geological map of the Polish part of the Carpathians based on Cieszkowski et al.,  
102 2017 and cited there, [faults after Lexa et al., 2000](#). **B:** [Main tectonic units under the Carpathians, after](#)  
103 [Żelaźniewicz et al., 2011](#).

105

106 **3.2 Analysis of the sectors**

107 We used the morphometry subdivision of Poland (Solon et al., 2018) to define the area, based on the  
 108 subprovinces of the Western Outer Carpathians in the area of Poland and a small band of Northern Subcarpathia  
 109 subprovince to the border of the Carpathians in the geological meaning (Carpathian overthrust on the Foredeep  
 110 sediments), according to Lexa et al. (2000). The subdivision of the outer Carpathian belt is mostly used in the  
 111 geology basis on the tectonostratigraphic units (nappes). This subdivision, however, does not allow differences  
 112 in lineament systems parallel to the belt to be caught. The newly proposed morphostructural subdivision of the  
 113 Western Carpathians (Minár et al., 2011) is another approach that compiles geological and morphological  
 114 features. The Polish part of the Western Carpathians is subdivided into the following subregions (number  
 115 according to the paper cited): (3f) Moravian–Silesian Beskid, (3a) Beskid Żywiecki–Gorce, (3b) Beskid  
 116 Sądecki–Levočské vrchy, (5a) Beskid Wyspowy, (5b) Low Beskid and (6) North Foreland. The last subregion  
 117 spans all the length of the northern Carpathian boundary between the Orava and San rivers. We decided to  
 118 compile the geological subdivision with the morphological one (Solon et al., 2018), which also comprises a  
 119 subdivision of the outermost units, into five sectors (Fig. 23, Tab. 1). The only change was including Mount  
 120 Ciecień Mount in Beskid Wyspowy into the Central Silesian sectors, as this massif, unlike all other Beskid  
 121 Wyspowy culminations is built of Silesian series deposits (Burtan, 1974).



122  
 123 **Fig. 23.** Sectors defined based on the physiogeographical (Solon et al., 2018) and tectonic subdivisions  
 124 (Golonka et al., 2020, 2021) of the study area (Western Outer Carpathians in Poland).

125  
 126 **Tab. 1.** Analyse sectors

Analyse sectors name;	Symbol	Mesoregions covered according to Solon et al., 2018
Western Silesian with Foremagura	WS	Silesian Beskid Mts., Żywiec Basin, Silesia Foothills, Mały Beskid Mts.
Central Silesian	CS	Wieliczka Foothills, Wiśnicz Foothills, Beskid

		Wyspowy Mts – only the Ciecień ridge, Rożnów Foothills, Ciężkowice Foothills, Gorlice Basin
Eastern Silesian and Skole	ES	Przemysł Foothills, Jasło-Krosno Basin, Strzyżów Foothills, Dynów Foothills, Jasło Foothills, Bukowiec Foothills
Western Magura	WM	Orawa-Jordanów Foothills, Orawa Interfluve, Koniaków Intermontane Region, Żywiec-Kysuce Beski, Pewel-Krzeczów Ranges, Makowski Beskid, Żywiec-Orawa Beskid
Central Magura	CM	Sącz Beskid Mts., Sącz Basin, Wyspowy Beskid (without Ciecień Ridge), Gorce Mts.
Eastern Magura and Dukla	EM	Low Beskid Mts.

127

128 **4. Data and methods**Digital elevation model

129 **4.1 — Digital elevation model**

130 The Global Multi-resolution Terrain Elevation Data 2010 (GMTED2010; see Danielson, 2011) 7.5 arc-second  
 131 product was chosen as a work base. The model is a compilation of different raster-based elevation sources, based  
 132 mainly on SRTM digital terrain elevation data. The resolution is ca. 0.0021°/pixel, which means ca. 233 m/pixel.  
 133 This was found to be sufficient, while the working scale during lineament detection was 1:150 000. As the  
 134 shading azimuth can influence the results, the working imagery was multidirectional hillshade ([Introducing](#)  
 135 [Esri's Next Generation Hillshade, 2022 Nagi, 2022](#)).

136 **5. Methods**

137 **4.25.1 Multiple cover lineament detection**

138 The manual method of lineament extraction was applied for two reasons. First, it is the simplest, low cost and  
 139 widely used method. The second reason is that it creates a basis for further work, based on automated extraction.  
 140 However, the method used is prone to some operator-related bias (Scheiber et al., 2015; Ehlen, 2004). Thus, to  
 141 reduce this bias the lineaments were extracted by two operators working independently, in three sessions,  
 142 separated by intervals of several months. After each session, the results were analysed and a network of common  
 143 features was created. Lineaments marked by both operators were merged into single feature. Lineaments marked  
 144 by only one operator were removed. The last stage was creating a concise network of lineaments based on the  
 145 results of the three sessions.

146

147 **4.35.2 Network analysis**

148 A network can be described by scale-independent topological characteristics, based on the case of a line network  
 149 on graph theory. The network (graph) is formed by nodes (end or intersection points) connected by lines  
 150 (Sanderson and Nixon, 2015; Mukherjee, 2019). The line can be formed by one or more branches connected by

Sformatowano: Nagłówek 1, Do lewej

151 nodes. The node can be isolated (I type), an embranchment (Y type) or an intersection (X type), where the latter  
152 two types are connecting nodes. Thus, the branch can connect two I type nodes (I-I branch), isolated and  
153 connecting nodes (I-C branch, which can be I-Y or I-X) and two connecting nodes (C-C branch, which can be  
154 X-X, X-Y or Y-Y). The proportion of nodes and branch types can be analysed as tertiary systems that  
155 characterise the properties of the network, especially its interconnectivity (Procter and Sanderson, 2018;  
156 Sanderson and Nixon, 2015; Sanderson et al., 2018).

157 The spatial variation of the topological parameters of the network was analysed with the following aspects: (1)  
158 regular, in a 5x5 km grid; and (2) within sectors based on the mesoregions of physiogeographical subdivision,  
159 according to Solon et al. (2018) and the main tectonic units (Fig. 2-3 Tab. 1).

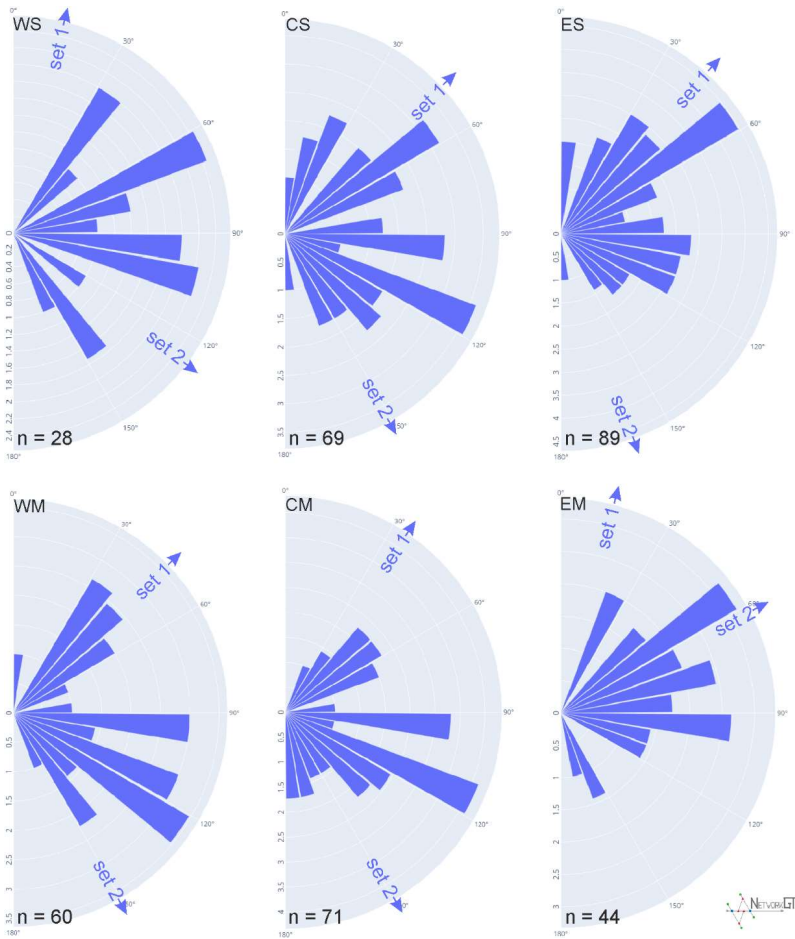
160 The NetworkGT Qgis toolbox (Nyberg et al., 2018) was used as a tool in the topological analyses. The lineament  
161 network was checked and repaired with NetworkGT tools. An additional stage was the manual correction of  
162 some features to eliminate all non-defined types of nodes, as well as some extremely short (ca. 500 m or shorter)  
163 features. The topological parameters were analysed in three modes: the whole network; the sectors defined; and  
164 in a regular, 5x5 km grid with 10 km search radius.

165 The Rayleigh test of semicircular distribution test was performed with the EZ-ROSE spreadsheet (Baas, 2000),  
166 and circular statistics were calculated with the SciPy stats module (The SciPy Community, 2022).

## 167 **5.6. Results**

### 168 **5.46.1 Network geometry**

169 The azimuths of the lineaments in all the analysed sectors show a multimodal distribution. Thus, the directions  
170 were separated into sets, in a way that gives low values of circular variance. The angular ranges of all the sets are  
171 presented in Tab. 2. For all sets, except for set 2 in the Eastern Magura (EM) sector and set 2 in the Western  
172 Silesian (WS) sector, the distribution is not uniform, as checked with the Rayleigh test (Baas, 2000). The two  
173 sets not checked were not numerous enough to be representative.



174  
 175 **Fig. 34:** Rose diagrams of the analysed networks in the analytic sectors; upper row: Western Silesia  
 176 **sector** with Foremagura (WS), Central Silesia (CS), Eastern Silesia **with Skole** (ES); lower row: Western  
 177 Magura (WM), Central Magura (CM), and Eastern Magura **with Dukla** (EM). Arrows mark the mean  
 178 azimuth for the sets defined in Tab. 2.

179  
 180 **Tab. 2.** Azimuths of the lineaments in the analyse sectors

Analyse sector	Set	Azimuths range	n	Circular statistics			The acute angle between sets means
				Mean	Std. dev	Variance	
CS	1	0 – 100	15	46.5	14.2	3.5	75.5
	2	100 – 180	13	151	16.6	4.8	



CM	1	0 – 80	17	34.1	13	3	63.9
	2	80 – 180	51	150.2	21.5	8.1	
EM	1	45 – 75	41	62.1	7.5	1.0	47.7
	2	0 – 45 75 – 180	3	14.4	26.7	12.5	
ES	1	0 – 100	59	42.7	19.7	6.8	62.1
	2	100 – 180	28	160.6	14.7	3.8	
WM	1	0 – 100	20	46.5	14.2	3.5	75.5
	2	100 – 180	40	151	16.6	4.8	
WS	1	0 – 60 150 – 180	23	13.6	23.3	9.5	66.2
	2	60 – 150	5	127.4	8.9	1.4	

181

182 The orientation of lineaments in all sectors, as well as the circular mean azimuth are shown in Fig. 34. In sectors  
183 Central and Eastern Silesian (CS, ES) and Central and Western Magura (CM, WM) the set 1 mean is located  
184 between 34° and 47°, marking a dominant SW–NE strike of lineaments. In the Western Silesian sector (WS), set  
185 1 is oriented more to the north (14°). In all sectors above, there is a second set with a NW–SE trend, mostly  
186 oriented at 150–160°, but in the Western Silesian sector case the mean azimuth is lower (127°), as in the case of  
187 the first set. The last sector, Eastern Magura and Dukla, is different. There is one dominant set with azimuth 62°,  
188 and the second set is poorly represented and oriented northward. The angle between the two sets varies in the  
189 62–76° range, except in the Eastern Magura and Dukla sector where it is only 48°.

### 190 5.26.2 Network topology

191 In the study area, 305 lineaments were marked in total. These features comprise 432 nodes. Of this count, 58%  
192 are I nodes, 19% are E nodes, 18% are Y nodes and 5% are X nodes. The network contains 338 branches, within  
193 which 49% are C–I type branches, 29% are C–C branches and 22% are I–I branches marking completely  
194 separated lineaments. Topological parameters are shown in Tab. 3.

195

196 **Tab. 3. Topological parameters of the network in analyse sectors**

	Western Silesian with Foremagura	Central Silesian	Eastern Silesian and Skole	Western Magura	Central Magura	Eastern Magura and Dukla	Whole area
	WS	CS	ES	WM	CM	EM	
No. of nodes (I+X+Y)	19	68	101	47	67	40	383
I nodes	8	51	76	26	48	36	293
X nodes	1	6	6	3	6	2	19
Y nodes	10	11	21	18	15	2	71
E nodes	22	38	49	46	61	52	-

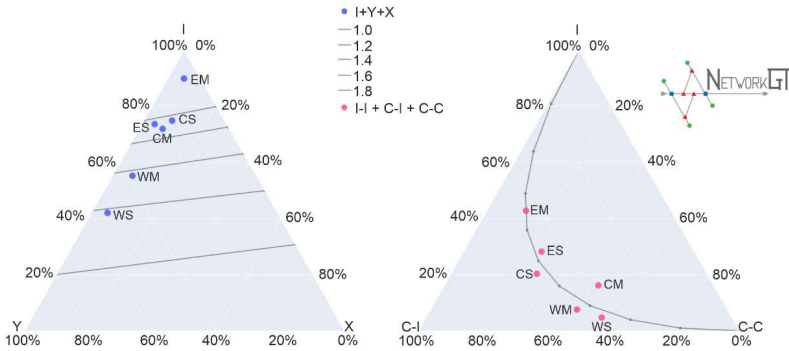
C-C connections	11.5	14.5	18.5	21.0	33.5	3.0	77.0
C-I connections	8.5	28.5	35.5	22.0	25.0	11.5	131.0
I-I connections	1.0	11.0	23.5	3.0	14.0	10.5	81.0
No. of branches	21.0	54.0	77.5	46.0	54.5	25.0	291
No. of lines	9.0	31.0	48.5	22.0	31.5	19.0	182
No. of connections	11	17	25	21	19	4	90
Connects per line	2.44	1.10	1.03	1.91	1.21	0.42	0.99
Connects per branch	1.62	1.06	1.02	1.43	1.12	0.56	0.99
Dim. less intensity	1.21	0.87	1.21	1.65	1.33	2.06	0.75
Av. Degree of network	2.21	1.59	1.53	1.96	1.63	1.25	1.52

197

198

199 The highest dimensionless intensity parameter is in the Eastern Magura and Dukla sector (2.05) and the lowest in  
200 the Central Silesian (0.87). On the other hand, the Eastern Magura sector is characterised by the lowest  
201 connections per branch (0.56) or the average degree of network (1.25) due to its form of mainly parallel features,  
202 with only 12% of the branches of connecting type (C–C). The best interconnectivity is observed in the Western  
203 Silesian sector with 1.62 connections per branch and an average degree of the network of 2.21. This is an effect  
204 of the presence of the Żywiec Basin block-system in the central part of the region.

205 The difference between these two (Eastern Magura and Western Silesia) sectors can be clearly visible on the  
206 ternary diagrams (Fig. 45) presenting the relationships of the nodes and branch types. In the Western Silesian  
207 sector, there is a high ratio of Y type nodes (52% of non-E-type nodes) and only one I–I branch.



208 **Fig. 45:** Ternary diagram presenting nodes (left) and branches (right) proportions in the analysed sectors.

209  
210  
211 The parameters of all the other sectors fall between the Eastern Magura and Western Silesian sectors. The  
212 Western Magura sector has quite good interconnectivity with a similar type of Eastern Magura blocky network.

213 Another approach to analysing topology is to use a sampling regular grid. The results are shown in Fig. 4-5 as  
214 maps of connections per branch number, 2D network intensity and dimensionless intensity.

215 It can be seen we have two relatively large regions with a high value of connections per branch parameter that in  
216 terms of connections per branch we have two relatively large regions with a high number. The first one is in the  
217 Western Silesian and partially Western Magura sectors, that is, the Żywiec Basin area, but from the geological  
218 point of view it is also a narrow zone of Foremagura units occurring between the Silesian and Magura nappes.  
219 Moreover, the Subsilesian unit tectonic window occurs in this area.

220 The Nowy Sącz Basin (eastern part of the Central Magura sector in the subdivision used here) is the next region  
221 with a high number of connections per network branch. The lineament system in this area surrounds a zone of  
222 Neogene deposits lying on the Carpathian flysch and filling the intramountain Nowy Sącz Basin.

223 The 2D intensity map shows that the Nowy Sącz Basin is characterised in general by a higher intensity than the  
224 Żywiec Basin. There is also a general trend of higher intensity in the western part of the Carpathians (especially  
225 the Western Magura and Central Magura sectors) than in the eastern part (Eastern Magura and Dukla).

226 In terms of dimensionless intensity parameter there are two regions with significantly high values: the south-  
227 eastern part of the Wiśnicz foothill, which is in the Central Silesian sector, and the eastern parts of the Beskid  
228 Niski Mts. and Bukowiec foothill in the Eastern Magura and Eastern Silesian sectors, on the geographical border  
229 of the Western and Eastern Carpathians.

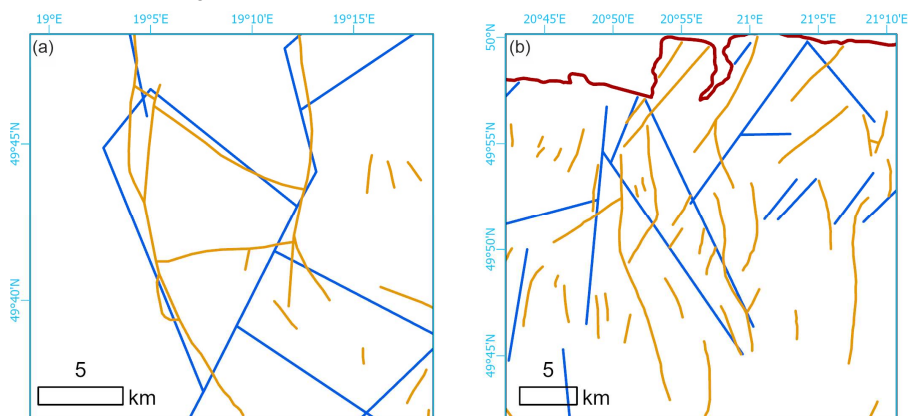
## 230 6.7. Discussion

### 231 6.7.1 Different lineament identification approaches

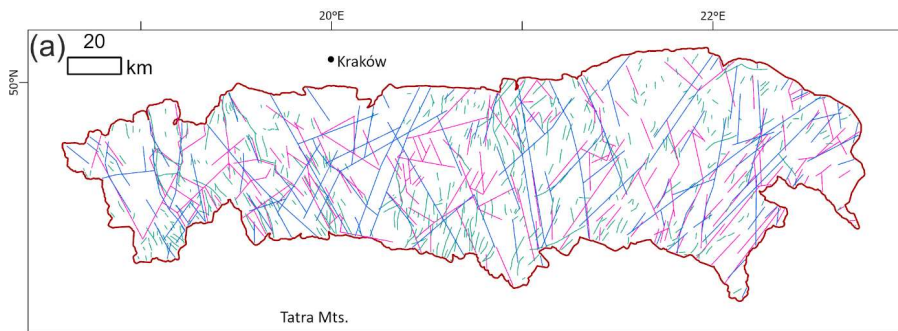
232 There are 110 photolineaments marked on the photogeological map of Poland in the studied area (Bażyński et  
233 al., 1986). In the same area of the geological map of the Carpathians, Lexa et al. (2000) marked 2 325 features  
234 described as a fault or assumed fault. In many cases, our lineament system seems to be concordant or  
235 complimentary to Lexa et al.'s (Fig. 56). In some cases, the features marked as faults are rather thrust lines, as  
236 per the Fig. 5a-6a example. The photolineament system is in general concordant with the DEM-interpreted

237 system. Visual inspection of the compiled lineaments map (Fig. 6a7a) shows that the especially NE striking  
 238 lineaments of the Eastern Magura sector are consistent with each other. Moreover, the system framing the  
 239 Żywiec tectonic window is well visible in both sets. On the other hand, there are some photolineaments that are  
 240 not recognisable on the DEM, and in fact also hardly visible on the modern orthophoto map. The most prominent  
 241 example are two straight, parallel lineaments striking the NNE in the central part of the study area, cutting its  
 242 entire width. These features seem to cut Gorcze Mts.; this is not confirmed by our other studies (Kania and  
 243 Szczęch, 2020; Szczęch and Cieszkowski, 2021). Further to the north, these two lineaments are delimiting  
 244 massifs of the Beskid Wyspowy Mts. (Mogielica, Łopień). These massifs are in fact particularly visible on the  
 245 aerial photo, as rather isometric "islands", and are formed by core parts of the synclines (Wójcik et al., 2009).  
 246 On the other hand, some lineament systems well visible in DEM are not marked on the photolineament map, as  
 247 per the case of the system north of the Nowy Sącz. That shows how these two methods can in fact be recognised  
 248 as complementary approaches to the lineaments' identification.

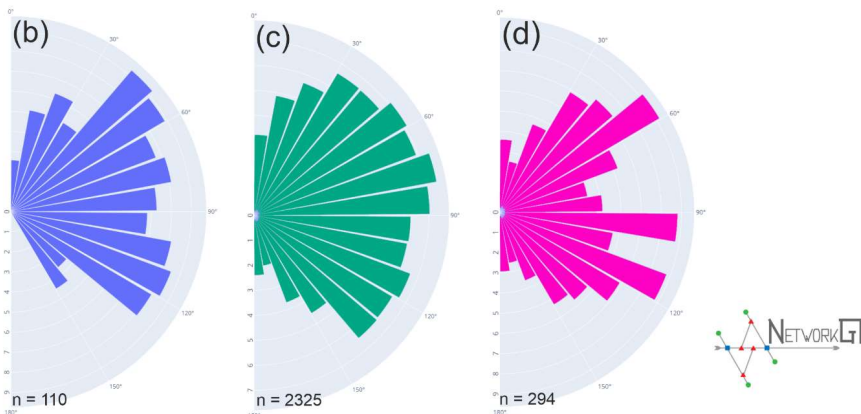
249 The system from the map by Lexa et al. (2000) shows confirmed and inferred faults, which is why it is not fully  
 250 compatible with lineaments; the lineaments, even when mainly tectonic related, are in fact a broader term  
 251 (O'Leary et al., 1976). Especially, these data, despite being a very rich collection of features are not applicable  
 252 for topological analyses: most of the features are short and isolated even when forming a network. Nevertheless,  
 253 these data include faults that are identified with geological criteria that are not visible in the remote sensing (at  
 254 least at the scale applied in this paper or by Bażyński et al., 1986 photolineament map. These data are  
 255 augmenting each other, which is highly visible in the Piwniczna Zdrój area, where DEM interpreted that the  
 256 NNW striking lineament along the Poprad River Valley (not present in the photolineament set) is flanked with a  
 257 set of N or NNE striking faults, which we have not identified on the DEM.



258  
 259 **Fig. 56.** Comparison of lineament system detected from the GMETD model (blue) and faults by Lexa et  
 260 al., 2000 (brown). (a) Żywiec Basin area, (b) fragment of the Zakliczyn – Olszyny fault zone.



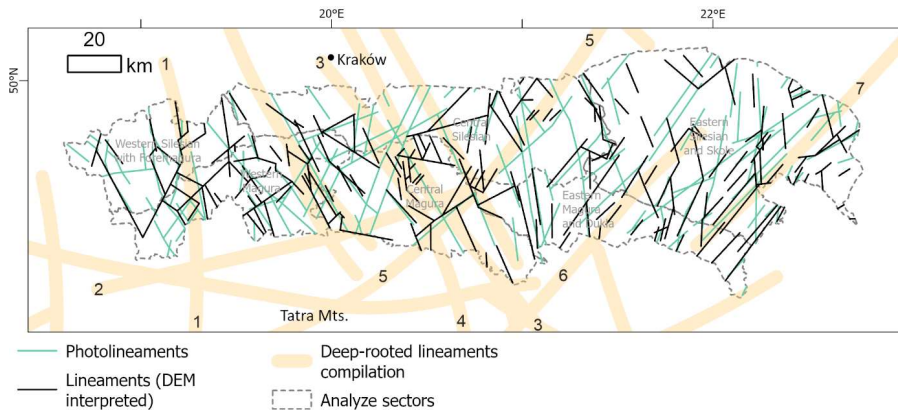
— Photolineaments by Bażyński et al., 1986    — Faults by Lexa et al., 2000    — Lineaments (DEM interpreted)



261  
 262 **Fig. 67. Geometry of lineament networks in the Carpathians. (a) compilation map of lineaments by**  
 263 **Bażyński et al., 1986, faults by Lexa et al., 2000 and lineaments interpreted from DEM in the presented**  
 264 **paper. (b-d) rosedigrams of features azimuth in the whole study area from: (b) Bażyński et al. (1986), (c)**  
 265 **Lexa et al., 2000 and (d) DEM interpreted.**

266  
 267 When analysing the distribution of feature azimuth for the whole study area (Fig. 667b-d), it can be noted that  
 268 the directions for the photolineament set (B) and DEM-interpreted set (D) are quite similar. What is noteworthy  
 269 is the lack of azimuths greater than 150° in the photo set, which are present (albeit in a minority) in the DEM set.  
 270 Furthermore, the photo set shows two maxima, at ca. 45° and 110°, whilst in the DEM set there are three  
 271 maxima at ca. 50°, 100° and 110°. However, the dominating directions are not in fact distributed uniformly  
 272 along the W–E span of the Polish Western Carpathians, which can be clearly seen in Fig. 6a–7a where the  
 273 domination of NE directions in the eastern sectors can be noticed, as well as the presence of two main directions  
 274 in the western and central sectors.





313  
314 **Fig. 78. Interpreted lineament system with photolineaments by Bażyński et al., 1986 as well as deep-rooted**  
315 **lineament compilation after Sikora, 1976; Zuchiewicz, 1984; Doktor et al., 1985. Important deep-rooted**  
316 **lineaments mark with numbers: 1 – Central Slovakia, 2 – Pericarpathian, 3 – Kraków – Prešov, 4 –**  
317 **Štítnik, 5 – Myjava, 6 – Muran, 7 - Przemyśl**

— sformatowano: Czcionka: Nie Pogrubienie

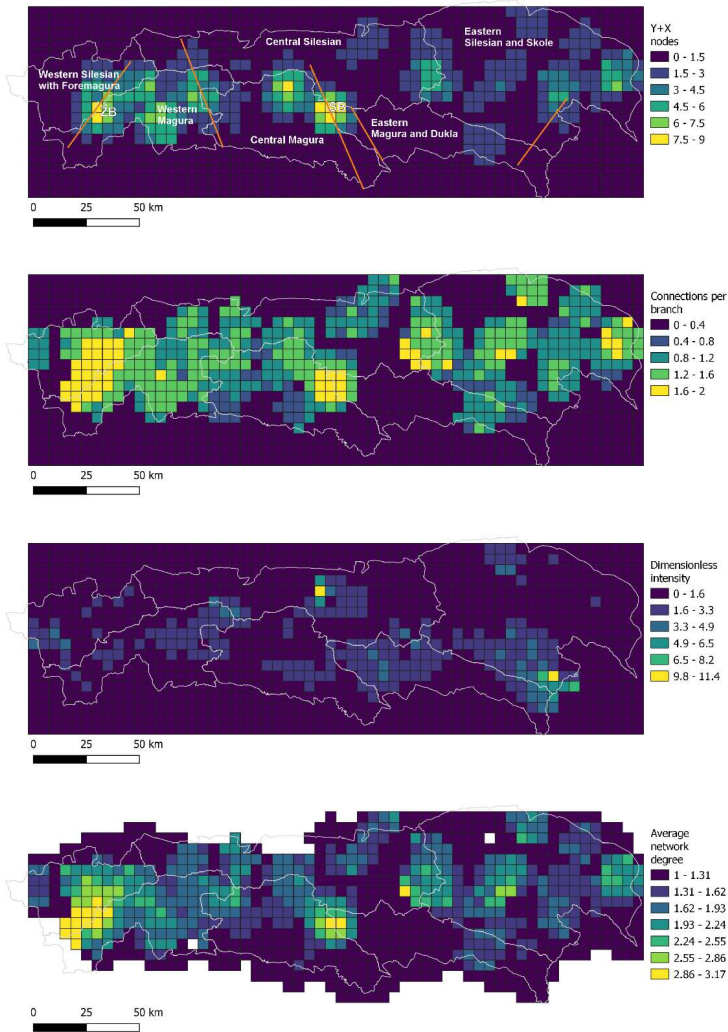
319 The central Slovak line marks the eastern border of the Żywiec basin and marks the major fault zone well visible  
320 in the displacing Fore-Magura belt near Żywiec. Some of the lineaments belonging to the system can also be  
321 traced to the east, with some connecting NE–SW branches near the northern margin of the Carpathians.

322 The system of Muran lineaments in the discussed region is marked by a few short NE–SW lineaments in the  
323 eastern sectors of the Magura and Silesian units. The Myjava system, in fact one of the most prominent systems  
324 in the Carpathians, in the study area can be traced along the Nowy Sącz Basin, continuing to the north where  
325 there is a series of short lines parallel to the zone lineaments. The network interconnectivity increases in this  
326 area. The lineaments there lie in an extension of the Carpathian Shear Corridor, a large-scale strike-slip zone  
327 between Vienna and the High Tatra Mts. (Marko et al., 2017). Although the Štítnik system is unclear, some  
328 parallel or subparallel lineaments can be assigned to this zone. The Przemyśl lineament zone is identified as a set  
329 of long lineaments in the easternmost parts of the area, where the main features of NE–SW are possibly  
330 interconnected by shorter N–S lines, forming an interconnected, blocky, two-set system.

331 Another important deep-rooted linear structure, confirmed by a negative gravimetric anomaly is the  
332 Pericarpathian line, which runs along the Nowy Sącz–Nowy Targ–Kysucké Nové Mesto line (Zuchiewicz, 1984;  
333 Sikora, 1976), which runs similarly to the Myjava structure. The Kraków–Prešov lineament, which is an  
334 extension of the Kraków–Lubliniec fault zone and marks the border between the Małopolska and  
335 Brunovistulicum blocks of the basement (Żaba, 1999; Zuchiewicz, 1984), runs along the Dunajec Valley. A  
336 system of lineaments is clearly visible along this line, mainly in the Magura Nappe; however, parallel  
337 photolineaments were marked even longer to the north (Bażyński et al., 1986).

339 These systems can be arranged in two sets: NNW, NW–SSE, SE striking (Central Slovakia, Skawa, Kraków–  
340 Presov and Štítnik); and NE–SE (Myjava and Pericarpathian, Muran and Przemyśl). That implies some points of  
341 system intersection, and in the area analysed such a place is in the Nowy Sącz region. This place is characterised

342 by higher interconnection factors (Fig. 89), in relation to the surrounding area. Moreover, in terms of  
 343 geomorphology, this is an intramountainous basin, being the only location where deposits are observed in the  
 344 Magura Nappe Neogene.



345  
 346  
 347 **Fig. 89.** Topological parameters of the lineament network, from up to down: connecting nodes number,  
 348 connections per branch number, dimensionless intensity factor, and average network degree. ZB – Żywiec  
 349 Basin (Żywiec tectonic window), SB – Nowy Sącz Basin, lines on X-Y, nodes map are main faults.

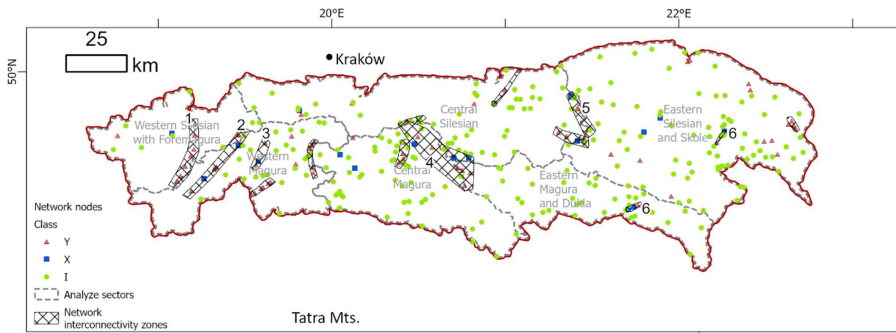
- sformatowano: Angielski (Zjednoczone Królestwo)
- sformatowano: Angielski (Zjednoczone Królestwo)
- sformatowano: Angielski (Zjednoczone Królestwo)



351 The Central Slovakian system strikes along the east border of the Żywiec Basin and Żywiec tectonic window,  
 352 where the Subsilesian Nappe is exposed. We also marked a major lineament there, which is not present on the  
 353 photolineament map (Bażyński et al., 1986) or the database of the Western Carpathian Geological Map (Lexa et  
 354 al., 2000). The lineament (in the central part, the Soła River Valley) cuts the Magura Nappe, the Foremagura  
 355 zone with Magura overthrust and the Silesian Nappe. This structure is one of the edges of the rhomboidal block,  
 356 in which the Żywiec Basin has been developed. The generally increased degree of network interconnection (Fig.  
 357 8|10) and the intensity of the network in this area can be an effect of the interaction between the central Slovakian  
 358 system with the Soła lineament and all the lowered block edges.

359 The cross-cutting relations of the Myjava lineament and the Štítník-Štítník lineament, whose continuation can be  
 360 the Dunajec fault system, are reflected in the bimodality of lineaments. The dominating maximum in the central  
 361 Magura sector, at approximately 120°, is similar to the Štítník-Štítník lineament; however, the Myjava lineament  
 362 is reflected there by just a few dominating lineaments, which are relatively long. Moreover, the Pericarpathian  
 363 lineaments are also known in this region. This structure, reflected in the sedimentary cover as the Dunajec fault  
 364 zone, is also confirmed by a negative gravimetric anomaly (Zuchiewicz, 1984; Sikora, 1976). Another deep  
 365 structure cutting this area is the Kraków–Prešov fault, which is an extension of the Kraków–Lubliniec fault  
 366 zone under the Carpathians active to the Quaternary (Żaba, 1999). All these deep cross-cutting features result in  
 367 an increased degree of the network connectivity observed on the surface. Then, the blocky structure allowed the  
 368 formation of an intramountain basin, filled with Neogene sediments.

369 Topological analysis also suggests that the well-known Skawa fault zone (Zuchiewicz et al., 2009; Unrug, 1980)  
 370 is in fact the western-most part of the wider zone of increased network interconnectivity, extending ca. 10–20 km  
 371 to the west of the Raba River. The final interpretation of correlation of lineaments increased interconnectivity  
 372 areas with tectonic structures of the area is shown on the Fig. 10.



374 **Fig. 10. Network nodes and zones of interconnectivity and their interpretation in context of Outer**  
 375 **Carpathians Nappes (surface) and basement (deep) tectonics. 1 – Soła fault zone (surface), Central**  
 376 **Slovakia lineament (deep), 2 – fault system along Sopotnia Valley, 3 – Skawa fault zone (surface), 4 –**  
 377 **Nowy Sącz Basin (surface), Kraków – Prešov, Myjava and Štítník lineaments (deep), 5 – faults along**  
 378 **Wisłoka Valley (surface), 6 – Muran lineament (deep),**

380

- Sformatowano:** Tabulatory: Nie w 3.09 cm
- **sformatowano:** Czcionka: Pogrubienie, Kolor czcionki: Tekst 1
- **sformatowano:** Czcionka: Pogrubienie, Kolor czcionki: Tekst 1, Angielski (Zjednoczone Królestwo)
- **sformatowano:** Czcionka: Pogrubienie, Kolor czcionki: Tekst 1
- **sformatowano:** Czcionka: Pogrubienie, Kolor czcionki: Tekst 1, Angielski (Zjednoczone Królestwo)
- **sformatowano:** Czcionka: Pogrubienie
- **sformatowano:** Czcionka: Pogrubienie, Angielski (Zjednoczone Królestwo)
- **sformatowano:** Czcionka: Pogrubienie, Angielski (Zjednoczone Królestwo)

381 The other aspect of the fault system of the Carpathians is occurrence and migration of the mineral waters. The  
382 area to the south of the Nowy Sącz there is a well-known region of CO<sub>2</sub>-rich mineral waters occurrence with  
383 renowned spa sites. These waters are associated with fault zones, often the deep one, penetrating to the  
384 crystalline basement of the Carpathians (Oszczytko and Zuber, 2002; Zuber and Chowaniec, 2009; Cieżkowski  
385 et al., 2010). Its noteworthy, that this region is located on the crossing of two major deep-rooted fault zones:  
386 Štitník lineament and Myjava lineament (Fig. 8). Similarly, the deep faults can be patch of migration of  
387 hydrocarbons, especially if source rocks are related to the platform cover of Brunovistulicum and Małopolska  
388 Massif lying under the Carpathians. In fact, some of the Polish Carpathian gas deposits are related to the  
389 Mesozoic-Palaeozoic basement (Kotarba and Koltun, 2006). Thus, the analyse of the fault systems and their  
390 interconnectivity has the potential in study of both, hydrocarbon and hydrogeological systems.

— sformatowano: Indeks dolny

### 391 **7.8. Conclusions**

392 The proposed data source and analysis method are complementary with other lineament analysis from the study  
393 area. The observed azimuths are in general concordant with the photolineament network; however, there are  
394 some structures that are not confirmed by DEM interpretation. The relationship between the DEM-interpreted  
395 data and geologically confirmed faults shows the usefulness of DEM as a data source in fault detection.

396 The dominating directions of the network are typical for the Western Carpathians, with a clear increase of the  
397 NE striking features proportion towards the east.

398 The topological properties of the lineament network in the Western Carpathians show E–W trends, but no clear  
399 S–N (perpendicular to the tectonic units) trends. This justifies the proposed subdivision of the Carpathians in the  
400 western, central and eastern sectors in addition to the tectono-facial subdivision. The eastern sectors are  
401 dominated by NE–SW trends and low interconnectivity, while the central and western sectors are more  
402 interconnected and characterised by cross-cutting relationships of two main lineament directions. The degree of  
403 network interconnectivity increases in areas with a lower morphology (intramountainous basins): the Żywiec  
404 Basin and Nowy Sącz Basin.

405 The geometry of the network, in general, reflects a system of deep-rooted lineaments. The cross-cutting area of  
406 the main deep lineaments is reflected in stronger network interconnectivity in the Nowy Sącz area.

407  
408 **CrediT authorship contribution statement:** Maciej Kania: Conceptualization, Methodology, Formal analysis,  
409 Investigation, Writing – original draft, Visualization. Mateusz Szczęch: Investigation, Writing – review &  
410 editing, Visualization.

411  
412 **Declaration of competing interest:** The authors declare that they have no known competing financial interests or  
413 personal relationships that could have appeared to influence the work reported in this paper  
414

415 **Acknowledgements:** The research was financed from funds of the Jagiellonian University Institute of  
416 Geological Sciences. Proofreading of this publication has been supported by a grant from the Priority Research  
417 Area (Digiworld) under the Strategic Programme Excellence Initiative at Jagiellonian University. The authors  
418 would like to thank both referees, Prof. Fabrizio Balsamo and Prof. Jan Golonka for their helpful comments  
419 improving a quality of the paper.

### 420 **References**

421 Baas, J. H.: EZ-ROSE: a computer program for equal-area circular histograms and statistical analysis of two-  
422 dimensional vectorial data, *Computers & Geosciences*, 26, 153–166, [https://doi.org/10.1016/S0098-](https://doi.org/10.1016/S0098-3004(99)00072-2)  
423 [3004\(99\)00072-2](https://doi.org/10.1016/S0098-3004(99)00072-2), 2000.

424 Bażyński, J., Doktor, S., and Graniczny, M.: Mapa fotogeologiczna Polski w skali 1:1 000 000, 1986.

425 [Burtan, J.: Detailed Geological Map of Poland, 1:50 000 scale, Mszana Dolna sheet, Wydawnictwa Geologiczne,](#)  
426 [Warszawa, 1974.](#)

427 Chodyń, R.: Zastosowanie cyfrowego modelu terenu (DEM) w badaniach geologicznych na przykładzie obszaru  
428 między Dobczycami a Mszaną Dolną (polskie Karpaty zewnętrzne), [Przegląd-Przegląd](#) Geologiczny, 52, 315–  
429 320, 2004.

430 Cieszkowski, M., Golonka, J., Waškowska-Oliwa, A., and Chrustek, M.: Budowa geologiczna rejonu Sucha  
431 Beskidzka – Świnna Poręba (polskie Karpaty fliszowe), *Geologia / Akademia Górniczo-Hutnicza im.*  
432 *Stanisława Staszica w Krakowie*, 32, 155–201, 2006.

433 Cieszkowski, M., Kysiak, T., Szczęch, M., and Wolska, A.: Geology of the Magura Nappe in the Osielec area  
434 with emphasis on an Eocene olistostrome with metabasite olistoliths (Outer Carpathians, Poland), *Annales*  
435 *Societatis Geologorum Poloniae*, 87, 169–182, <https://doi.org/10.14241/asgp.2017.009>, 2017.

436 [Cieźkowski, W., Chowaniec, J., Górecki, W., Krawiec, A., Rajchel, L. and Zuber, A.: Mineral and thermal](#)  
437 [waters of Poland. \*Przegląd Geologiczny\*, 58, 762–773, 2010.](#)

438 Danielson, J. J.: Global Multi-resolution Terrain Elevation Data 2010 (GMTED2010) Coastal Elevation  
439 Modeling View project LP DAAC View project, 2011.

440 Doktor, S. and Graniczny, M.: Geologiczna interpretacja zdjęć satelitarnych i radarowych wschodniej części  
441 Karpat, *Kwartalnik Geologiczny*, 26, 231–245, 1982.

442 Doktor, S. and Graniczny, M.: Fotogeologiczna analiza zdjęć satelitarnych Karpat, *Kwartalnik Geologiczny*, 27,  
443 645–656, 1983.

444 Doktor, S., Dornic, J., Graniczny, M., and Reichwalder, P.: Structural elements of Western Carpathians and their  
445 Foredeep on the basis of satellite interpretation, *Geological Quarterly*, 29, 129–138, 1985.

446 Doktor, S., Graniczny, M., Kucharski, R., Molek, M., and Dąbrowska, B.: Wgłębna budowa geologiczna Karpat  
447 w świetle kompleksowej analizy teledetekcyjno-geofizycznej, *Przegląd Geologiczny*, 38, 469–475, 1990.

448 Doktor, S., Graniczny, M., Kowalski, Z., and Wójcik, A.: ~~Możliwości~~ ~~Możliwości~~ zastosowania wyników  
449 interpretacji ~~zdjęć~~ ~~zdjęć~~ radarowych do analizy tektonicznej Karpat, *Przegląd-Przegląd* Geologiczny, 50, 852–  
450 860, 2002.

451 Ehlen, J.: Lincation, edited by: Goudie, A. S., *Encyclopedia of Geomorphology*, 2, 623–624, 2004.

452 Golonka, J., Aleksandrowski Paweł and Aubrecht, R., Chowaniec, J., Chrustek, M., Cieszkowski, M., Florek, R.,  
453 Gawęda, A., Jarosiński, M., Kępińska, B., and others: The Orava deep drilling project and post-palaeogene  
454 tectonics of the northern Carpathians, *Annales Societatis Geologorum Poloniae*, 75, 211–248, 2005.

455 Golonka, J., Waškowska, A., and Ślącza, A.: The Western Outer Carpathians: Origin and evolution, *Zeitschrift*  
456 *der Deutschen Gesellschaft für Geowissenschaften*, 229–254, 2019<sup>a</sup>.

— sformatowano: Angielski (Zjednoczone Królestwo)

— sformatowano: Polski

— sformatowano: Angielski (Zjednoczone Królestwo)

457 Golonka, J., Waškowska, A., and Ślącza, A.: The western outer carpathians: Origin and evolution, *Zeitschrift*  
458 *der Deutschen Gesellschaft für Geowissenschaften*, 170, 229–254, <https://doi.org/10.1127/zdgg/2019/0193>,  
459 2019b.

460 Golonka, J., Gawęda, A., and Waškowska, A.: Carpathians, Reference Module in Earth Systems and  
461 Environmental Sciences, in: Alderton, D. and Elias, S. A. (eds.): *Encyclopedia of Geology (Second Edition)*,  
462 Academic Press, 4372–40381, <https://doi.org/10.1016/b978-0-12-409548-9.12384-x>, 20202021.

463 Graniczny, M. and Mizerski, W.: Lineamenty na zdjęciach satelitarnych Polski – próba podsumowania,  
464 *Przegląd Geologiczny*, 51, 474–482, 2003.

465 Kania, M. and Szczęch, M.: Geometry and topology of tectonolineaments in the Gorce Mts. (Outer Carpathians)  
466 in Poland, *J Struct Geol*, 141, 104186, <https://doi.org/10.1016/j.jsg.2020.104186>, 2020.

467 Kania, M. and Szczęch, M.: Tectonic Structures Interpretation Using Airborne-Based LiDAR DEM on the  
468 Examples from the Polish Outer Carpathians, in: *Atlas of Structural Geological and Geomorphological*  
469 *Interpretation of Remote Sensing Images*, edited by: Misra, A. A. and Mukherjee, S., 157–165, 2022.

470 Kotarba, M. J., and Koltun, Y. V.: The Origin and habitat of hydrocarbons of the Polish and Ukrainian parts of the  
471 Carpathian Province, in: Golonka, J. and Picha, F., *The Carpathians and Their Foreland: Geology and*  
472 *Hydrocarbon Resources: AAPG Memoir*, 84, 321–368, 2006.

473 Książkiewicz, M.: The Tectonics of the Carpathians, in: *Geology of Poland*, vol. 4. Tectonics. The Alpine  
474 Tectonic Epoch, Geological Institute, Warszawa, 476–608, 1977.

475 Leech, D. P., Treloar, P. J., Lucas, N. S., and Grocott, J.: Landsat TM analysis of fracture patterns: A case study  
476 from the Coastal Cordillera of northern Chile, *Int J Remote Sens*, 24, 3709–3726,  
477 <https://doi.org/10.1080/0143116031000102520>, 2003.

478 Lexa, J., Bezák, V., Elečko, M., Mello, J., Polák, M., and Vozár, J.: Geological map of western Carpathians and  
479 adjacent areas 1:500 000, 2000.

480 Mahel', M.: Tectonics of the Carpathian–Balkan Regions, Explanations to the Tectonic Map of the Carpathian–  
481 Balkan Regions and Their Foreland., Štátny geologický ústav Dionýza Štúra, Bratislava, 180–197 pp., 1974.

482 Marko, F., Andriessen, P. A. M., Tomek, Č., Bezák, V., Fojtíková, L., Bošanský, M., Piovarči, M., and  
483 Reichwalder, P.: Carpathian Shear Corridor – A strike-slip boundary of an extruded crustal segment,  
484 *Tectonophysics*, 703–704, 119–134, <https://doi.org/10.1016/j.tecto.2017.02.010>, 2017.

485 Van der Meer, F. D., van der Werff, H. M. A., van Ruitenbeek, F. J. A., Hecker, C. A., Bakker, W. H., Noomen,  
486 M. F., van der Meijde, M., Carranza, E. J. M., de Smeth, J. B., and Woldai, T.: Multi- and hyperspectral geologic  
487 remote sensing: A review, <https://doi.org/10.1016/j.jag.2011.08.002>, 2012.

488 Minár, J., Bielik, M., Kováč, M., Plašienka, D., Barka, I., Stankoviansky, M., and Zeyen, H.: New  
489 morphostructural subdivision of the Western Carpathians: An approach integrating geodynamics into targeted  
490 morphometric analysis, *Tectonophysics*, 502, 158–174, 2011.

491 Motyl-Rakowska, J. and Ślącza, A.: Ważniejsze lineamenty *karpát-Karpat* i ich związek ze znanymi *uskokami*,  
492 *Przegląd Geologiczny*, 32, 72–77, 1984.

— sformatowano: Angielski (Zjednoczone Królestwo)

— sformatowano: Angielski (Zjednoczone Królestwo)

— sformatowano: Angielski (Zjednoczone Królestwo)

493 Mukherjee, S.: Using Graph Theory to Represent Brittle Plane Networks, 259–271,  
494 <https://doi.org/10.1016/B978-0-12-814048-2.00022-3>, 2019.

495 [Nagi, R.](https://www.esri.com/arcgis-blog/products/arcgis-living-atlas/imagery/introducing-esri-next-generation-hillshade/): Introducing Esri's Next Generation Hillshade: [https://www.esri.com/arcgis-blog/products/arcgis-living-atlas/imagery/introducing-esri-next-generation-hillshade/?rmedium=redirect&rsorce=blogs.esri.com/esri/arcgis/2014/07/14/introducing-esri-next-generation-hillshade](https://www.esri.com/arcgis-blog/products/arcgis-living-atlas/imagery/introducing-esri-next-generation-hillshade/), last access: 1 June 2022.

499 Nyberg, B., Nixon, C. W., and Sanderson, D. J.: NetworkGT: A GIS tool for geometric and topological analysis of two-dimensional fracture networks, *Geosphere*, 14, 1618–1634, <https://doi.org/10.1130/GES01595.1>, 2018.

501 O'Leary, D. W., Friedman, J. D., and Pohn, H. A.: Lineament, linear, lineation: Some proposed new standards for old terms, *Geological Society of America Bulletin*, 87, 1463–1469, 1976.

503 Oszczytko, N.: Late Jurassic-Miocene evolution of the Outer Carpathian fold-and-thrust belt and its foredeep basin (Western Carpathians, Poland), *Geological Quarterly*, 50, 169–194, 2006.

505 [Oszczytko, N. and Zuber, A.: Geological and isotopic evidence of diagenetic waters in the Polish Flysch Carpathians, \*Geologica Carpathica\*, 53, 257–268, 2002.](#)

507 Ozimkowski, W.: Lineamenty otoczenia Tatr - porównanie interpretacji DEM i MSS, *Przegląd Geologiczny*, 56, 1099–1102, 2008.

509 Plaśienka, D.: Continuity and episodicity in the early Alpine tectonic evolution of the Western Carpathians: How large-scale processes are expressed by the orogenic architecture and rock record data, *Tectonics*, 37, 2029–2079, 2018.

512 Procter, A. and Sanderson, D. J.: Spatial and layer-controlled variability in fracture networks, *J Struct Geol*, 108, 52–65, <https://doi.org/10.1016/j.jsg.2017.07.008>, 2018.

514 Sanderson, D. J. and Nixon, C. W.: The use of topology in fracture network characterization, *J Struct Geol*, 72, 55–66, <https://doi.org/10.1016/j.jsg.2015.01.005>, 2015.

516 Sanderson, D. J., Peacock, D. C. P., Nixon, C. W., and Rotevatn, A.: Graph theory and the analysis of fracture networks, *J Struct Geol*, 14th April, <https://doi.org/10.1016/j.jsg.2018.04.011>, 2018.

518 Scheiber, T., Fredin, O., Viola, G., Jarna, A., Gasser, D., and Łapińska-Viola, R.: Manual extraction of bedrock lineaments from high-resolution LiDAR data: methodological bias and human perception, 137, 362–372, <https://doi.org/10.1080/11035897.2015.1085434>, 2015.

521 Sikora, W.: On lineaments found in the Carpathians, [Annales Societatis Geologorum Poloniae Rocznik Polskiego Towarzystwa Geologicznego](#), 46, 3–37, 1976.

523 Ślęczka, A., Kruglov, S., Golonka, J., Oszczytko, N., and Popadyuk, I.: Geology and hydrocarbon resources of the Outer Carpathians, Poland, Slovakia, and Ukraine: general geology, in: [Golonka, J. and Picha, F.](#), The Carpathians and [their Their forelandForeland](#): Geology and [hydrocarbon-Hydrocarbon resourcesResources](#): AAPG Memoir, 84, 221–258, 2006.

527 Solon, J., Borzyszkowski, J., Małgorzata Bidłasik, Richling, A., Badora, K., Balon, J., Brzezińska-Wójcik, T., Chabudziński, Ł., Dobrowolski, R., Grzegorzczak, I., Jodłowski, M., Kistowski, M., Kot, R., Krąż, P., Lechnio,

— sformatowano: Angielski (Zjednoczone Królestwo)

— sformatowano: Polski

529 J., Macias, A., Majchrowska, A., Malinowska, E., Migoń, P., Myga-Piątek, U., Nita, J., Papińska, E., Rodzik, J.,  
530 Strzyż, M., Terpiłowski, S., Ziaja, W., and Paul, J.: Physico-geographical mesoregions of Poland: verification  
531 and adjustment of boundaries on the basis of contemporary spatial data, *Geographia Polonica*, 91, 143–170,  
532 <https://doi.org/10.7163/GPol.0115>, 2018.

533 Szczęch, M. and Cieszkowski, M.: Geology of the Magura Nappe, south-western Gorce Mountains (Outer  
534 Carpathians, Poland), *Journal of Maps*, 17, 453–464, <https://doi.org/10.1080/17445647.2021.1950579>, 2021.

535 Teisseyre, W.: O związku w budowie tektonicznej Karpat i ich przedmurza, *Kosmos*, 32, 393–402, 1907.

536 Statistics (scipy.stats) — SciPy v1.9.3 Manual: <https://docs.scipy.org/doc/scipy/tutorial/stats.html>, last access: 8  
537 November 2022.

538 Thiele, S. T., Jessell, M. W., Lindsay, M., Ogarko, V., Wellmann, J. F., and Pakyuz-Charrier, E.: The topology  
539 of geology 1: Topological analysis, *Journal of Structural Geology*, 91, 27–38,  
540 <https://doi.org/10.1016/J.JSG.2016.08.009>, 2016.

541 Unrug, R.: Tectonic rotation of flysch nappes in the Polish Outer Carpathians, *Rocznik Polskiego Towarzystwa*  
542 *Geologicznego*, 50, 27–39, 1980.

543 Valentini, L., Perugini, D., and Poli, G.: The “small-world” topology of rock fracture networks, *Physica A:*  
544 *Statistical Mechanics and its Applications*, 377, 323–328, <https://doi.org/10.1016/j.physa.2006.11.025>, 2007.

545 Wójcik, A., Czerwiec, J., and Krawczyk, M.: Szczegółowa Mapa Geologiczna Polski 1:50 000. arkusz  
546 Limanowa, 2009.

547 Yang, L., Meng, X., and Zhang, X.: SRTM DEM and its application advances,  
548 <https://doi.org/10.1080/01431161003786016>, 2011.

549 [Żaba, J.: Ewolucja strukturalna utworów dolnopaleozoicznych w strefie granicznej bloków górnośląskiego i](#)  
550 [małopolskiego, \*Prace Państwowego Instytutu Geologicznego\*, 166, 1–162, 1999.](#)

551 [Zuber, A. and Chowanec, J.: Diagenetic and other highly mineralized waters in the Polish Carpathians, \*Applied\*](#)  
552 [Geochemistry](#), 24, 1889–1900, 2009.

553 Zuchiewicz, W.: The late Neogene - Quaternary tectonic mobility of the Polish West Carpathians - a case study  
554 of the Dunajec drainage basin, *Annales Societatis Geologorum Poloniae*, 54, 133–189, 1984.

555 Zuchiewicz, W., Tokarski, A. K., Świerczewska, A., and Cuong, N. Q.: Neotectonic Activity of the Skawa River  
556 Fault Zone (Outer Carpathians, Poland), *Annales Societatis Geologorum Poloniae*, 79, 67–93, 2009.

557 [Żaba, J.: Ewolucja strukturalna utworów dolnopaleozoicznych w strefie granicznej bloków górnośląskiego i](#)  
558 [małopolskiego, \*Prace Państwowego Instytutu Geologicznego\*, 166, 1–162, 1999.](#)

559 [Żelaźniewicz, A., Aleksandrowski, P., Buła, Z., Kornkowski, P. H., Konon, A., Oszczytko, N., Ślaczka, A.,](#)  
560 [Żaba, J. and Żytko, K.: Regionalizacja Tektoniczna Polski. Komitet Nauk Geologicznych PAN, Wrocław, 1–60](#)  
561 [pp., 2011.](#)

562

563

— sformatowano: Angielski (Zjednoczone Królestwo)

— sformatowano: Angielski (Zjednoczone Królestwo)

— sformatowano: Polski

— sformatowano: Polski